Chapter 19
Determining the Optimal Battery Model for a Specific Application

Bogdan-Adrian Enache

Abstract Determining the optimal battery model for a specific application is a complex process that must take into account several factors: the type of application, the accuracy required, the degree of complexity, etc. This chapter introduces a new method for determining the optimal model and has its starting point in analyzing the discharge profile, and employs a multi-criteria analysis for processing the experimental data. The method presented is validated experimentally for a $LiFePO_4$ battery subjected to discharge after an Urban Dynamometer Driving Schedule (UDDS) cycle.

Abbreviation and Acronyms

BMS	Battery Management System
DC	Direct Current
LFP	$LiFePO_4$ battery
MCA	Multi-Criteria Analysis
OCV	Open Circuit Voltage
PCB	Protection Circuit Board
RC	Resistance–Capacitor
SoC	State of Charge
SoH	State of Health
UDDS	Urban Dynamometer Driving Schedule

19.1 Introduction

In order to operate, electric vehicles, just like mobile devices, require the energy stored in their batteries. The limitations on the amount of energy that can be stored, as well as the limitations concerning safe operation, restrict the employability of

B.-A. Enache (✉)
Faculty of Electronics, Communications and Computers, University of Pitesti, Pitesti, Romania
e-mail: b0gdan.enache@yahoo.com

N. Bizon et al. (eds.), *Energy Harvesting and Energy Efficiency*, Lecture Notes in Energy 37, DOI 10.1007/978-3-319-49875-1_19

batteries within certain, very strict limits. Battery operation within these limits is the responsibility of the Protection Circuit Board (PCB) that equips the battery. Further developments of the PCB were made in order to extend is applicability not only to safety issues but also to better energy efficiency and so the Battery Management System (BMS) was born.

These devices receive as input the operating parameters of the battery, and based on the logic that they implement, ensure the extraction of the maximum capacity of the battery within the boundaries specified by the manufacturer. Due to the complex processes that occur within the battery, some of these parameters, such as State of Charge (SoC) and State of Health (SoH), cannot be measured directly. However, these characteristics are critical for the energy efficiency of the battery, therefore they must be assessed by a different method. Currently, the most widely used method for determining the SoC and SOH is by approximating them based on a model of the battery operation. By embedding such a model into the BMS a significant improvement in battery capacity during discharge is achieved [1].

The main strategies of developing a functional model of the battery are the electrochemical approach and the approach oriented towards electric circuits, but there are also models that combine elements of both strategies.

The electrochemical models are based on the description of the processes occurring within the battery. They are used to explain the electrochemical phenomena occurring when the electrode interacts with the electrolyte [2]. Therefore they make use of differential equations systems with several unknowns. Using a computer to solve the equation systems gives rise to algebraic loops that need approximation methods to remove them and also to reduce the number of parameters involved. The big advantage of the electrochemical models is their high accuracy. Using such a model in [3] is obtained, for a Li-ion battery, an error smaller than 0.01% to approximate the SoC.

The models based on circuits use electrical and electronic components to describe the behaviour of the battery subjected to discharge. They have as a common source the *Rint* (*elementary*) *model*, which is composed only of a DC voltage source and a resistor set in series. Starting from this, other models have been developed by adding parallel resistor-capacitor branches. The accuracy of the most popular models based on electric circuits is analyzed in [3] which reports for a $LiMn_2O_4$ battery that is subjected to discharge at constant current a maximum relative error in determining the SoC between 0.1 and 0.35%. Unlike the electrochemical models, the models based on electric circuits have lower accuracy, but their easy development and implementation makes them ideal for incorporation into simulation programs.

The analytical models are models that combine properties of the electrochemical models and of the models based on circuits. Their aim is to develop a model that contains a small number of equations and a high accuracy, while at the same time being easy to use in other programs.

Because of the fact that models are being developed along three different directions, choosing the optimal model is a complex issue, which must take into

account many factors, of which the most important are: the scope of the application, the degree of accuracy and the time required to make the model.

In order to develop a BMS for portable devices, where the accuracy of the model used is not the most important parameter, but rather the ability to run in real-time on embedded systems, simple models based on electric circuits are the ideal solution [4, 5].

As far as the applications for electronic devices in which the main factor of interest is displaying the SoC for the user, the models based on electric circuits compete with the analytical ones, as the discriminating factor is their computational complexity.

On the other hand, the sole viable solution for the hybrid vehicles applications designed to reduce fuel consumption, to determine the car performance, or improve the parameters of the batteries, which are usually carried out offline and require high accuracy, are the electrochemical models [3].

The recommendations listed above are general, and are only useful so far as the categorization of the model is concerned, and not for choosing the model itself.

In order to determine the optimal battery model for a specific application a new method based on the analysis of the discharge profile and the use of a multi-criteria analysis (MCA) is presented. This methodology, which is the main contribution of this chapter, was developed for better BMS development and it combines energy efficiency with ease of implementation. The proposed methodology is best suited for Li-Ion batteries which present highly non-linear evolution of the SoC and other parameters.

Li-ion batteries are currently the most common type for power the mobile electronic devices and electric cars. The best known structures of these batteries are: $LiCoO_2$, $LiMn_2O_4$, $LiNiO_2$, $LiNiMnCoO_2$, $LiNiCoAlO_2$, $LiFePO_4$, and they combine high energy density with high power density. Their main disadvantage is related to the flat plateau area from the discharge characteristic which makes very difficult the determination of the SoC [6]. Among these batteries the $LiFePO_4$ (LFP) ones, which use a graphite anode and a cathode made of Li ferrophosphate distinguish them self. The olivine structure of the cathode gives these batteries a high structural and thermodynamic stability, making them the safest Li-based batteries [7]. Besides the advantages of safety and the fact that their structure does not contain rare metals (Ni, Co, Mn, etc.), LFP batteries also present a set of negative aspects as compared to the rest of Li-Ion batteries. The most important of them are the low energy density, the low electrical potential (3.2–3.3 V compared to 3.6–3.7 V that is typical for Li-Ion batteries) and the strongly non-linear discharge characteristic.

The next of the chapter is organized as follows: Sects. 19.2–19.4 describe the most known types of modeling strategies—electrochemical, analytical and circuit based followed by the proposed screening process for determining the optimal model for a specific application and a case study to validate it.

19.2 Electrochemical Models

The electrochemical models describe the behaviour of batteries based on the chemical processes that occur between the electrodes and the electrolyte. They use a set of differential equations to represent, in time, the processes of ion diffusion, transportation, reduction, oxidation, and distribution, and the side effects occurring in the battery. Solving these equations yields the time evolution of the battery voltage and current.

The complexity of the chemical processes determines the complexity of the model, and thus the number of differential equations needed for it.

There are several electrochemical models, which, starting from the lumped model which needs only two equations, evolve towards the very complex models that require up to six equations and more than 50 parameters in order to describe the behaviour of the battery.

19.2.1 The Lumped Model

The lumped model was one of the first models that described the processes that take place in the battery with a less complex chemical structure, such as lead-acid batteries or some Ni-MH batteries.

This model is based on the Butler-Vormer equations and the Nerst theory, and considers the spatial distribution of the chemical elements between the two electrodes as uniform.

In this model the Open Circuit Voltage (OCV) generated by the electrochemical processes is given by the Nerst equation [3]:

$$\Phi(t) = \Phi^0 - \frac{RT}{nF} \ln\left(\prod_k \left(m_k(t)\gamma_k\right)^{\nu_k}\right) \tag{19.1}$$

where:

- $\Phi(t)$—the potential of an electrode [V];
- Φ^0—the electromotive force under standard conditions [V];
- R—the universal gas constant;
- T—temperature [K];
- F—Faraday's constant [C/mol];
- k—number of participants in the reaction;
- m—molarity;
- γ—the activity coefficient;
- ν—stoichiometric ratio

To determine the current density of the battery the Butler-Vormer equation is used [2]:

$$J(t) = J_0 \left[e^{\frac{\alpha F}{RT}\eta(t)} - e^{\frac{(1-\alpha)F}{RT}\eta(t)} \right] \tag{19.2}$$

where:

- J_0—density of transfer current;
- α—transfer coefficient;
- η—polarization.

The advantage of this model is that it uses only two simple equations, which are easy to integrate in a simulation software. Thus, a model was developed for a Ni-MH cell, which allowed simulating its behavior in a matter of milliseconds by using the existing computers [4].

The main disadvantage of the lumped model is that the equations that it uses are insufficient to describe the complex processes taking place in the modern batteries, which use advanced materials such as Li-ion, Li-Po, metal-air, etc. To model such batteries a new class of models has been developed, which have as a starting point the porous electrode theory. Among these the best known model is the Doyle-Fuller-Newman model which is presented next.

19.2.2 The Doyle–Fuller–Newman Model

The Doyle-Fuller-Newman model describes in detail the electrochemical processes of ion diffusion, transport and distribution that take place into a Li-ion battery. The structure of a Li-ion cell—Fig. 19.1, consists of an anode and a cathode made from a porous material, which are isolated by a separator, the whole assemblage being immersed in the electrolyte.

When the battery is charged, the *Li* ions occupy the interstitial space within the anode. As the battery discharges, the *Li* ions leave the anode and enter the electrolyte. From there they pass through the separator and reach the cathode. This migration of ions ends when they reach the cathode and occupy an interstitial space within it. When *Li* ions leave the anode, an electron is released into the external circuit, generating power. When that electron reaches the cathode, it allows a *Li* ion to occupy a position inside it. Charging retraces the *Li* ions path, yet backwards, and now the cell receives power from the external circuit cell instead of delivering electricity.

The Doyle-Fuller-Newman is also known as the 1D model because it considers the dynamic processes as taking place only along one axis (the horizontal axis—*x*). This approximation is made because the length of a cell structure along the *x*-axis is

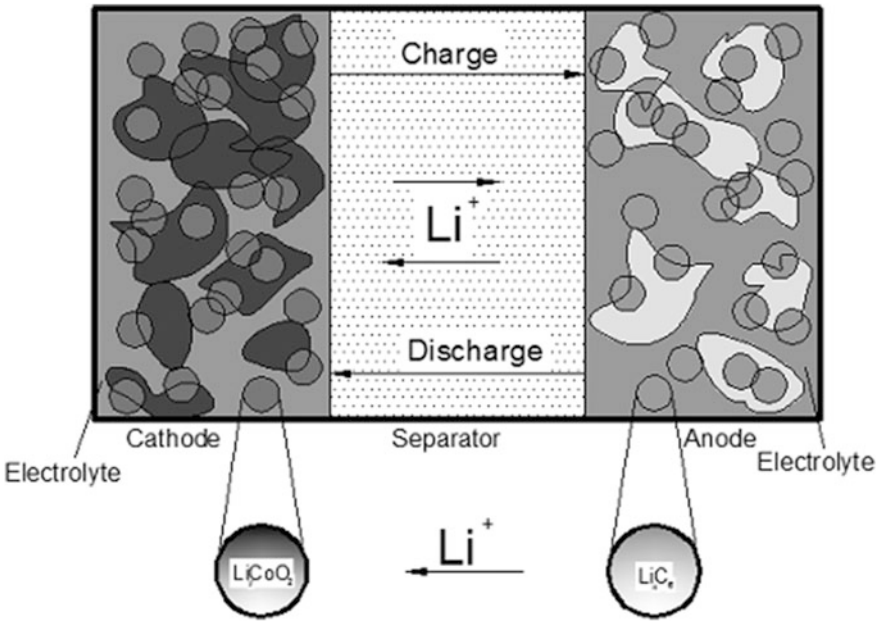

Fig. 19.1 Structure of a Li-Ion cell [2]

much smaller (of the order of 100 μm) than the length of the structure for the other axes (ranging up to 100,000 μm) [3].

The model uses a set of differential equations to describe the linear diffusion of *Li* ions in the electrolyte and the solid material of the electrodes, as well as the spatial distribution of the electrochemical processes generated as part of that process. These equations are obtained from Fick's diffusion law (for *Li* ion concentration), Ohm's law (for electric potential distribution) and the Nerst and Butler-Vormer equations [8]. The coefficients occurring in these equations are listed in Table 19.1.

The 1D model is based on the diffusion of *Li* ions in the solid material of the electrodes. This diffusion occurs at each point of the anode and the cathode, and is modelled by the following equation, where the particles taking part in the reaction are considered to be spherical [9].

$$\frac{\partial c_{1,j}}{\partial t}(r,t) = \frac{d_{1,j}}{r^2}\frac{\partial}{\partial r}\left(r^2\frac{\partial c_{1,j}}{\partial r}(r,t)\right) \tag{19.3}$$

Table 19.1 Symbols used for the Doyle–Fuller–Newman model

Symbol	Name	U.M.
L_n	Thickness of the anode	m
L_s	Thickness of the separator	m
L_p	Thickness of the cathode	m
R_n	Radius of anode particles	m
R_p	Radius of cathode particles	m
t^+	Transfer number	–
b	Brugman's number	–
d_2	Diffusivity of solution	m^2s^{-1}
ε_{2n}	Fractional volume of the anode solution	–
ε_{2s}	Fractional volume of the separator solution	–
ε_{2p}	Fractional volume of the cathode solution	–
d_{1n}	Diffusivity of anode solid material	m^2s^{-1}
d_{1p}	Diffusivity of cathode solid material	m^2s^{-1}
k_n	Anode reaction rate	$(Am^{-2})\ (mol\ m^{-3})^{1+\alpha}$
k_p	Cathode reaction rate	$(Am^{-2})\ (mol\ m^{-3})^{1+\alpha}$
R_{SEI}	Thickness of the anode layer	m
c_2	Concentration of the initial solution	$mol\ m^{-3}$
u_{nref}	Anode balance potential	V
u_{pref}	Cathode balance potential	V
k	Solution conductivity	Ωm

On the other hand, the concentration of *Li* ions in the electrolyte—$c_2(x,t)$, depends on the current density J and is described by Fick's law [9]:

$$\varepsilon_2 \frac{\partial c_2}{\partial t}(x,t) = \frac{\partial}{\partial x}\left(d_2^{eff}\frac{\partial c_2}{\partial t}(x,t)\right) + \frac{1-t^+}{F}J(x,t) \tag{19.4}$$

The current density J is determined by the potential difference between the electrolyte solution and the solid material of the electrodes, and is, according to the Butler-Vormer relationship [9]:

$$J(\mathrm{x},t) = a_j i_{0,j}\left[e^{\frac{\alpha_{a,j}F}{RT}\eta_j(\mathrm{x},t)} - e^{-\frac{\alpha_{c,j}F}{RT}\eta_j(\mathrm{x},t)}\right] \tag{19.5}$$

$$i_{0,j} = k_j\left(c_{1,j}^{\max} - c_{1,j}^{S}\right)^{\alpha_{a,j}}\left(c_{1,j}^{S}\right)^{\alpha_{c,j}}(c_2)^{\alpha_{a,j}}, j = n,p \tag{19.6}$$

The electrochemical potential of the two electrodes, including both the solid material and the electrolyte solution, is described mathematically by the relations [9]:

$$\begin{cases} \eta_p(x,t) = \phi_1(x,t) - \phi_2(x,t) - u_{pref}(x,t) \\ \eta_n(x,t) = \phi_1(x,t) - \phi_2(x,t) - u_{nref}(x,t) - \frac{J(x,t)}{a_n}R_{SEI} \end{cases} \tag{19.7}$$

Considering Ohm's law, the potential for each component of the electrodes can be determined by means of the relationships [9]:

$$\frac{\partial}{\partial x}\left(\sigma_j^{eff}\frac{\partial \phi_{1,j}}{\partial x}(x,t)\right) - J(x,t) = 0 \tag{19.8}$$

$$\frac{\partial}{\partial x}\left(k^{eff}\frac{\partial \phi_2}{\partial x}(x,t)\right) + J(x,t) + \frac{\partial}{\partial x}\left(k_D\frac{\partial}{\partial x}\ln(c_2(x,t))\right) = 0 \tag{19.9}$$

The differential equations system (19.3)–(19.9) represents the 1D model for a cell Li-ion cell that is both in the process of discharging and in the process of recharging.

The traditional methods for solving this equations system are based on the finite difference technique, which consists in dividing the x axis into equal intervals that are small enough to allow estimation of derivatives using Taylor series.

Another way to process it is by linearization and solving the equations using the BAND subroutine [10]. This subroutine is coded in COBOL and solves nonlinear of equations systems with partial derivatives. The subroutine underlay the development of the DUALFOIL software, which is used for modelling and simulation of complex-structure batteries.

19.2.3 DUALFOIL

DUALFOIL is a free software, coded in FORTRAN, which enables modelling and simulation of such batteries as Lithium-metal, Li-ion, Na-ion and Ni-MH.

To be used, the program requires an input file with the specific parameters of the battery being modelled. The user must enter in this file, in addition to the battery discharge profile, no less than 50 parameters concerning its geometrical and electrochemical properties. Among them are the thickness and porosity of the electrodes, the initial temperature, salt concentration in the electrolyte, heat dissipation capacity for the entire battery, diffusion coefficient, etc. [10].

After running, the program produces four output files. The main file contains the values for the most important parameters: time, current, voltage and battery temperature. The remaining files contain more detailed reports about the battery operating mode; the most important being the file that describes the evolution of internal resistance.

In order to be used, the DUALFOIL program requires detailed knowledge about the battery to be modelled, which is not always accessible to the average user. But once this obstacle has been overcome, the results of the modelling are of high fidelity, and are often used as benchmarks for determining the accuracy of other models.

The electrochemical models are based on a linear equations system that describe the electrochemical phenomena that takes place inside the batteries. To solve this

system, a whole range of techniques of simplification and approximation are used, which do not significantly affect the accuracy of the model, but do not reduce its complexity, either. Electrochemical models generally have a high accuracy, yet they require long periods of time for simulation and detailed knowledge about the electrochemical structure of the batteries that are being modelled. For this reason they cannot be incorporated into other simulation systems that include other functional elements apart from batteries.

To facilitate incorporation of the battery model within a more general simulation system electrochemical models have been abandoned for models whose accuracy is smaller, while also being less complex. These models were grouped into two classes: analytical models, and models based on electric circuits.

19.3 Analytical Models

Analytical models describe the behaviour of the battery at a higher level of abstraction than electrochemical models. They have been developed from experimental tests performed on the battery, and the obtained data were processed by curve fitting techniques. The great advantage of these models is that they manage to describe the behaviour of the battery using a small number of equations. The best known analytical models are the Shepherd model and the Peukert model which are presented next.

19.3.1 The Peukert Model (Peukert's Law)

Wilhelm Peukert studied the behaviour of lead-acid batteries subjected to constant current discharge. Following these tests, he noticed that only one equation is sufficient to determine the remaining battery capacity for a discharge current:

$$C = I^k \cdot t \tag{19.10}$$

where:

- C—battery capacity, expressed in Ah;
- I—discharging current;
- t—discharge time, in hours;
- k—calibration coefficient.

Equation 19.10 is known as Peukert's law, and was developed to model the behaviour of the battery for different discharge currents.

When a battery is subjected to discharge using increasingly higher constant currents, it was found that the battery internal resistance increases and the discharged battery capacity (up to the cutoff voltage) decreases. To compensate for

these losses Peukert introduced the calibration coefficient k, also known as Peukert's coefficient.

The value of Peukert's coefficient is determined experimentally using two different battery discharge curves. If we consider that the battery is discharged in time t_1 for the current I_1, and in t_2 for the current I_2, then, applying Eq. (19.10), one gets:

$$\left.\begin{aligned} C &= I_1^k \cdot t_1 \\ C &= I_2^k \cdot t_2 \end{aligned}\right\} \Rightarrow I_1^k \cdot t_1 = I_2^k \cdot t_2 \Rightarrow \left(\frac{I_1}{I_2}\right)^k = \frac{t_2}{t_1} \Rightarrow$$
$$k \cdot \ln\left(\frac{I_1}{I_2}\right) = \ln\frac{t_2}{t_1} \Rightarrow k = \frac{\ln\frac{t_2}{t_1}}{\ln\left(\frac{I_1}{I_2}\right)} \tag{19.11}$$

Introducing the calibration coefficient was only a partial solution for determining the capacity discharged from the battery. It has been experimentally proven that, in a battery subjected to discharge under a high value current, even after the cutoff voltage is reached, the available capacity it is not zero [11]. This remaining capacity is caused by the decrease of the active centers number in the active substance at the cathode and the rapid increase in the resistance for the interaction between the anode and the electrolyte [12, 13].

Similarly, it was demonstrated experimentally that the Peukert model can only be applied to batteries that are subjected to discharge at constant current and constant temperature. In many real situations, however, the battery discharge is done using varying currents within an extended temperature range. In such circumstances, the Peukert model usually approximates a smaller capacity for the battery [11].

A first attempt to adapt the Peukert model, when the discharging current is variable, involves using an effective pseudo-current. Thus the discharge alternating current is discretized in several areas where its value can be considered constant; and for those areas the value of the pseudo-current (I_{eff}) is calculated, using the relationship:

$$I_{eff} = I \cdot \left(\frac{I}{I_{nom}}\right)^{k-1} \tag{19.12}$$

where I is the constant discharge current, I_{nom} is the rated discharge current supplied by the manufacturer (usually, a battery discharge time of 20 h).

In this situation the total discharged capacity (C_d) from the battery is determined for each constant current range (Δt) as:

$$C_d = \sum \left(I_{eff} \cdot \Delta t\right) \tag{19.13}$$

This method is generally accepted as an improvement on the Peukert model [14] for variable currents; however its accuracy is limited because it neglects the temperature effects over the discharge.

Another way to improve the Peukert model proposes an equation that includes the effects of both a variable current and the temperature variation. Accordingly, the capacity discharged from the battery is defined as:

$$\Delta C_d = f(I, T) \tag{19.14}$$

Considering the least favorable case, when the discharging temperature drops and the current increases, in order to describe the behaviour of the variable discharge current this relationship is used:

$$f(I) = \left(\frac{I}{I_{nom}}\right)^{\alpha} \tag{19.15}$$

where α is a constant that depends on the type of the calibration coefficient.

To describe the behaviour of the temperature within the discharge process, a function similar to that presented in (19.15) is used.

$$f(T) = \left(\frac{T_{nom}}{T}\right)^{\beta} \tag{19.16}$$

where: T_{nom} is the rated discharge temperature, T is the temperature in the discharge process, and β is a coefficient that depends on the battery technology and the battery configuration.

Considering the relations (19.15) and (19.16), an improved Peukert model is given by:

$$\Delta C_d = \gamma \cdot \left(\frac{I}{I_{nom}}\right)^{\alpha} \cdot \left(\frac{T_{nom}}{T}\right)^{\beta} \tag{19.17}$$

where γ is a coefficient that compensates the combined effect of α and β coefficients.

This model has been verified experimentally, and it was shown to have an error of less than 5% for an extended range of temperature and discharge currents [14].

The Peukert model is one of the simplest and most enduring models developed to simulate battery behaviour. Although it has undergone some changes over time, it remains a model with a limited degree of accuracy, which is used, in particular, to deal with batteries with a simple structure. For batteries that involve more complex phenomena in the process of discharge, the Peukert model is not sufficient. For such batteries a different model that combines ease of use with high accuracy, namely the Shepherd model is used.

19.3.2 The Shepherd Model

The Shepherd model was developed to optimize the capacity/weight ratio of the batteries used by the US Navy. To achieve this objective it was considered necessary to develop a model that could express the dependence of the output voltage of the battery for a specific the discharge [15].

Developing the model was done according to the following hypotheses:

- The anode and cathode have porous active materials;
- The electrolyte and the electrodes are homogeneous;
- The electrodes are parallel;
- The current density is evenly distributed between the two electrodes;
- The distance between the electrodes is small compared with their dimensions (width, length);
- The temperature is constant;
- Internal resistance is constant;
- The battery is discharged at a constant current.

After formulating the hypotheses, the development of the model passed on obtaining the discharge curves for different types of batteries: Ni-Cd, silver-zinc-alkaline; Air-zinc-alkaline, lead-acid, etc. On this basis Shepherd noted that any discharge feature presents three distinct areas which are presented in Fig. 19.2 and are:

- The initial area;
- The zone determined by the polarization effects;
- The zone determined by internal resistance;

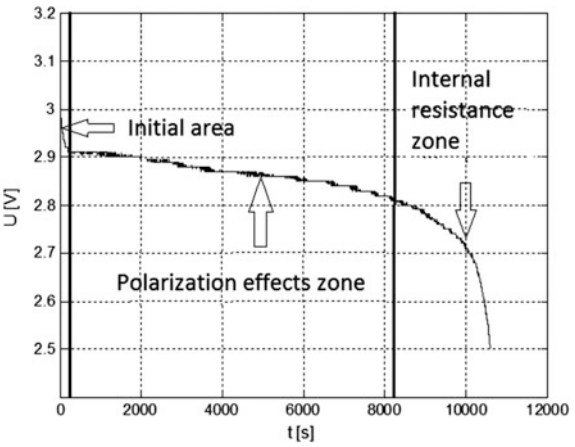

Fig. 19.2 The discharge zones for a $LiFePO_4$ battery

After establishing the discharge zones, Shepherd approximated their evolution by a series of curves with known equations. As a result of this process, it was determined that the equation that best models the discharge behavior of the battery is:

$$V_{batt} = E_0 - K \cdot \left[Q / \left(Q - \int idt \right) \right] \cdot i - R_0 \cdot i \tag{19.18}$$

where:

- V_{batt}—output voltage of the battery (V);
- E_0—open circuit voltage (V);
- K—polarization coefficient (Ω);
- Q—battery capacity (Ah);
- i—discharge current (A)
- R_0—battery internal resistance (Ω).

This relationship is known as the Shepherd model. It presents a nonlinear term $K \cdot \left[Q / \left(Q - \int idt \right) \right]$ that models the terminal voltage variation in accordance with the magnitude of the discharge current. This behaviour is specific to real batteries, but this term generates an infinite loop and instability in simulation [16].

For the Shepherd model to be usable in simulations software, the algebraic loop must be removed. The models obtained in this way are known as simplified Shepherd models, and the most representative such model is described by the relation [17]:

$$V_{batt} = E_0 - K \cdot [Q/(Q - i \cdot t)] + A \cdot \exp(-B \cdot it) \tag{19.19}$$

where:

- A—the amplitude at the end of zone 1 (V);
- B—the inverse value of the capacity discharged at the end of zone 2 (Ah^{-1}).

The Shepherd model has the great advantage of incorporating, into a single equation, the dependence of output voltage for a discharge current. This makes it easy to use in a complex simulation system that also includes other operation equations for the components involved.

As regards the simulation systems that use electrical and electronic components, the Shepherd model, and by extension analytical models, cannot be used, so a new category of models was developed specifically for these systems, i.e. models based on electric circuits which are presented next.

19.4 Models Based on Electric Circuits

The models based on circuits describe the electrochemical phenomena that occur as part of the batteries, using only electrical and electronic components. They typically use voltage sources, resistors and capacitors to model the variation of the output voltage for a specific discharge current and SoC.

The complexity of the system is given, in general, by the number of components used in the model. The simplest systems use only a voltage source and a resistor, and the most complex ones use in addition one or more parallel resistor—capacitor branches.

19.4.1 The Elementary (Rint) Model

The simplest circuit model used to describe the behaviour of a battery consists of a voltage source whose value is equal to the OCV of the battery (E_0) and a resistance whose value is equal to the internal resistance of the battery (R_0)—Fig. 19.3.

If a load is connected to the terminals of that circuit, it will produce a current in the circuit which, according to Kirchhoff's second theorem, will have the expression:

$$I = \frac{E_0 - V_{batt}}{R_0 + R_L} \tag{19.20}$$

where V_{batt} is the output voltage, and R_L is the load resistance.

The emergence of the discharge current will lead to a lower battery capacity, and consequently to a output voltage drop. To model this behaviour it is necessary that both the value of the supply voltage and the value of the internal resistance should change in concordance with the battery SoC. This being the case, the easiest method for determining the remaining battery capacity consists in integrating the

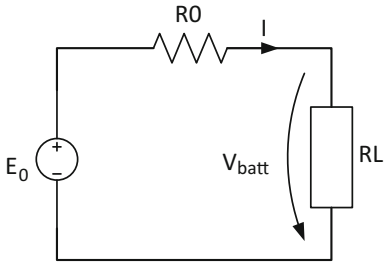

Fig. 19.3 The elementary (Rint) model

discharge current over time. Thus, by integrating Eq. (19.20) one gets the variation of the SoC for a specific discharge current:

$$SOC(t) = SOC(t_0) - \frac{1}{Q_{NOM}} \int_{t_0}^{t} I(t)dt \tag{19.21}$$

where:

- $SOC(t)$—the battery charge status at a given time t;
- $SOC(t_0)$—the battery charge status at the beginning of the discharge;
- Q_{NOM}—rated capacity of the battery;
- I—discharge current.

In those specific cases where the battery charge state is very well determined, the discharge current has very low variance, and the discharge time is also short, the elementary model is sufficient to accurately model the behaviour of the battery.

The elementary model considers the battery to be an ideal voltage source whose value depends only on the discharge current and SoC, but it fails to consider more complex phenomena such as polarization or hysteresis, and therefore in the more complex simulations its accuracy is limited.

A way for increasing the elementary model's accuracy in incorporating a number of nonlinear elements to reproduce the more complex phenomena occurring in the battery. One of these models is the Thévenin model.

19.4.2 The Thévenin Model

It is a circuit-based model, which extends the elementary model by adding a parallel group consisting of a resistor and a capacitor (an RC branch)—Fig. 19.4.

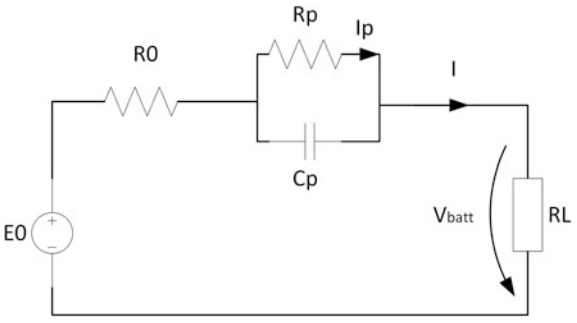

Fig. 19.4 The Thévenin model

Applying Kirchhoff's second theorem for the Thévenin, one gets:

$$V_{batt} = E_0 - R_0 \cdot I - R_p \cdot I_p \tag{19.22}$$

where R_p is the polarization resistance and I_p is the polarization current.

The polarization current is obtained by applying Kirchhoff's first theorem to the circuit node and taking into account the expression of the current on the polarization capacitor C_p side:

$$\frac{dI_p}{dt} = \frac{(I - I_p)}{\tau} \tag{19.23}$$

where $\tau = R_p C_p$ is the time constant of the circuit.

A discrete solution of the Eq. (19.23) is [18]:

$$I_{p,i} = \left(1 - \frac{1 - \exp(-\Delta t/\tau)}{-\Delta t/\tau}\right) \cdot I_i + \left(1 - \frac{1 - \exp(-\Delta t/\tau)}{-\Delta t/\tau}\right) \cdot I_{i-1} + \exp(-\Delta t/\tau) \cdot I_{p,i-1} \tag{19.24}$$

Keeping the same discretization pace and applying the solution provided by Eq. (19.24) in the Eq. (19.22), the equation for the Thévenin model is obtained in a discrete form:

$$V_{batt,i} = E_0 - R_0 \cdot I_i - R_p \cdot I_{p,i} \tag{19.25}$$

This Eq. (19.25) is the basis for determining the values of the components used in the model. The main techniques for extracting the parameters of the model are based on the analysis of a discharge pulse or approximation and errors minimizing strategies.

The Thévenin model is able, by adding the RC branch, to model both polarization effects and the effects of the loss of capacity due to the high current discharge [3]. From this point of view it manages to describe some of the complex processes that occur within the battery without appealing to complicated differential equations.

The Thévenin model combines the electrochemical effects occurring into the batteries with the ease of use and easy integration into simulation systems, which makes it a model often used both by battery manufacturers and developers of systems for the automotive industry.

19.4.3 The R-C Network Model

It is a model that extends the Thévenin model by adding several parallel resistance–capacitor branches—Fig. 19.5. The number of RC branches models the transitory behaviour of the battery through a truncated exponential series. They determine, in fact, the resolution of the system response for various input signals.

For a real battery there are no exponential series that can entirely model its behaviour, therefore the number of RC branches must be chosen in such a way as to best approximate the behaviour of the battery for a particular discharge profile [18].

By applying Kirchhoff's first theorem to each node of the RC networks and taking into account that the voltage on an RC branch is the same for both the capacitor and the resistor, one can obtain the differential equation of the system:

$$\begin{bmatrix} \dot{V}_{C1} \\ \dot{V}_{C2} \\ \vdots \\ \dot{V}_{Cn} \end{bmatrix} = \begin{bmatrix} -\frac{1}{R_1 C_1} & 0 & \dots & 0 \\ 0 & -\frac{1}{R_2 C_2} & \dots & 0 \\ 0 & 0 & \dots & -\frac{1}{R_n C_n} \end{bmatrix} \cdot \begin{bmatrix} V_{C1} \\ V_{C2} \\ \vdots \\ V_{Cn} \end{bmatrix} + \begin{bmatrix} \frac{1}{C_1} \\ \frac{1}{C_2} \\ \vdots \\ \frac{1}{C_n} \end{bmatrix} \cdot i \qquad (19.26)$$

where V_{C1}, V_{C2}, ... V_{Cn} represent the voltages over the branches RC_1, RC_2, ... RC_n, R_1, R_2, ... R_n—the resistances in the RC branches, C_1, C_2, ... C_n—the capacity of the capacitors of the RC branches, and i the discharge current.

By solving the Eq. (19.26), and considering Kirchhoff's second theorem, the equation of the RC network model is obtained:

$$V_{batt} = E_0 - R_0 \cdot I - V_{C1} - V_{C2} - \cdots - V_{Cn} \qquad (19.27)$$

where E_0 is the OCV who dependents on SoC, and R_0 the internal resistance.

The parameters to be determined for the use of this model are: E_0 function of SoC, R_1, R_2, … R_n respectively C_1, C_2, … C_n.

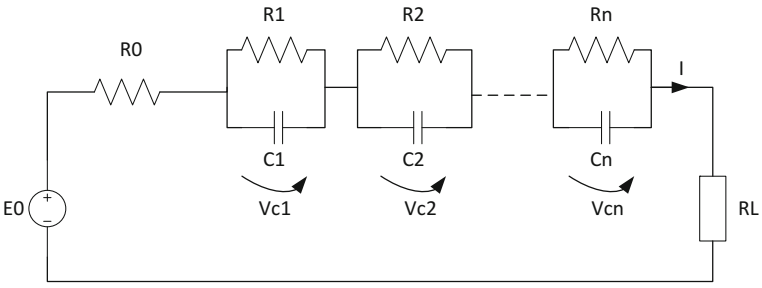

Fig. 19.5 The RC network model

19.5 Determining the Optimal Battery Model for a Specific Application

Determining the optimal battery model for a specific application is actually a problem of establishing a compromise between accurately approximating the experimental data and the complexity of the model. In general, the complexity of the model is limited by the computational resources and the correlation of the phenomena occurring inside the battery with the number of elements that are part of it [19].

Another indispensable factor that needs to be taken into account when determining the optimal model is the nature of the discharge profile. As a result of experimental measurements carried out in [20] it is shown that in discharge profiles involving rapid current changes, the response of the system is determined by the component with the lowest time constant.

In general the most common discharge profiles is the constant current discharge [21, 22] or slow variation pulses [23]. For this case, the determination of the optimal model is done by analyzing the response of the system to a discharge impulse at 10% of the SoC [21]. This method of analysis cannot be applied in the case of complex profiles that include rapid variations of the discharge current.

Taking into account all of the above, next is presented a novel method for determining the optimal battery model for a specific application. This method comprises of two phases: a discharge profile analysis and a data processing stage for choosing the model that combines best approximation of the experimental data with the minimum of resources used.

In the first stage from the discharge profile are extracted the areas that have rapid variations of the discharge current and the areas where the discharge current is constant, namely plateau areas. Since a single model should best approximate both areas, the less favorable ones are extracted. These areas are the area where the variation of the discharge current occurs within the shortest period of time, and the area where the plateau discharge has the longest period. For those areas the response speed of the models undergoing analysis will be determined.

In the second stage the experimental data previously obtained are processed by a MCA and the optimal model is determined.

MCA is a tool for comparison and ranking of the different results, even when using multiple evaluation criteria [24]. It operates with several concepts, of which the most important are: the option, the criteria, the performance matrix, the score and weight.

The **options** are items that are subject to comparison or hierarchy. Of these, after applying the MCA, the best solution (option) is chosen according to certain criteria.

A **criteria** is the measure according to which the options are assessed. Each criteria measures a relevant aspect of the option, and should not depend on any other criteria.

Systematization of data, as part of the MCA, is done by using the **performance matrix**. Each row of the matrix represents option, and each column includes an

evaluation criteria. The values that are recorded in each cell represent the performance level of an option for a particular evaluation criteria.

The **score** (the number of **points**) represents the value of the consequences generated by each option. They are usually standardized for a scale between 0 and 100, where the best option gets 100, and the remaining options get values proportional to their performance.

The **weights** represent a percentage values assigned to each criteria in order to highlight its importance. The sum of the weights must add up to 100%.

In the next section a case study which involve determining the optimal model for a LFP battery subjected to discharge after the Urban Dynamometer Driving Schedule (UDDS) cycle is presented. This study has the main goal of establishing the best suited model to be incorporated into a BMS for a LFP battery. The model has to combine ease of implementation with energy efficiency.

The characteristics of the LFP cell used are:

- Rated voltage: 3.3 V
- Rated discharge current: 0.7 A
- Rated capacity: 1400 mAh for the rated discharge current
- Cut off voltage: 2.5 V
- Maximum allowable discharge current: 2.1 A.

The UDDS discharge cycle—Fig. 19.6, was chosen because of its high complexity [25] and also because it is part of the basic tests aimed to determine the characteristics of the batteries that equip electric and hybrid cars in Europe and America, alongside other test such as: European Driving Cycle, Extra Urban Driving Cycle, Highway Fuel Economy Test, New York City Cycle, Urban Dynamometer Driving Schedule.

To determine the optimal model for the LFP cell subjected to discharge after the UDDS cycle only those models which include the variation of the output voltage with the discharge current, and which can be incorporated in a BMS will be

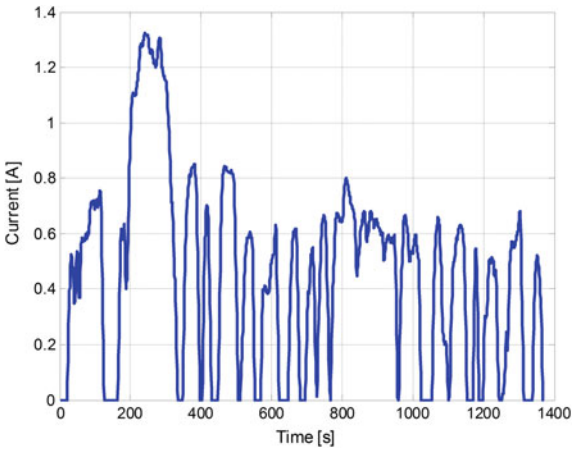

Fig. 19.6 The UDDS discharge cycle

Table 19.2 The parameters of the Shepherd model

	E_{FULL} (V)	E_{EXP} (V)	Q_{EXP} (Ah)	E_{NOM} (V)	Q_{NOM} (Ah)
Shepherd	3.430	3.409	0.068	3.301	1.120

analyzed. Therefore, the following models were chosen: Shepherd, Thévenin, second, third and fourth RC network.

Determining the parameters used in these models was based on experimental tests carried out in accordance with the procedures prescribed in the USABC [26], and PNGV [27, 28], manuals. The determined parameters are presented in Tables 19.2 and 19.3.

In accordance with the method proposed, in the first stage the UDDS discharge cycle is analyzed, and the most representative areas of rapid change and plateau are extracted—Fig. 19.7a. These areas are number from P1 to P5 for the plateau areas and from R1 to R6 for the rapid change ones, after this they are organized according to their duration. The longest plateau and the shortest rapid change areas are chosen which, in this case, are P3 and R2. From these areas a new discharge profile is constructed—Fig. 19.7b.

This profile is applied to the selected models and their response speed for the two areas is calculated—Fig. 19.8.

The second stage of the proposed methodology is dedicated to data analysis. Now the MCA for the five models is constructed as follows:

Options: The Shepherd model, the Thévenin model, the RC network model of order II, III and IV;

Criteria: The response speed of the models for the new discharge profile (for both areas P3 and R2) and the number of parameters needed for the modelling (to reduce the complexity of the models).

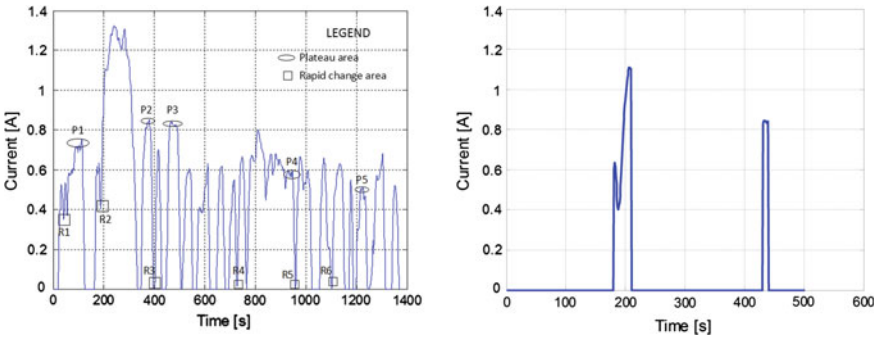

(a) Determining the areas of interest

(b) The new discharge profile

Fig. 19.7 Analysis of the UDDS discharge cycle

Table 19.3 The parameters of the models based on electric circuits

	E_0 (V)	R_0 (Ω)	R_1 (Ω)	C_1 (F)	R_2 (Ω)	C_2 (F)	R_3 (Ω)	C_3 (F)	R_4 (Ω)	C_4 (F)
Thévenin	3.313	0.131	0.053	337.1	–	–	–	–	–	–
Second order RC	3.313	0.131	0.038	257.5	0.014	549.4	–	–	–	–
Third order RC	3.313	0.131	0.038	257.5	0.005	549.4	0.008	549.4	–	–
Fourth order RC	3.313	0.131	0.038	257.5	0.005	549.4	0.003	549.4	0.004	549.4

Weights: Response rates for both areas get a 45% weight, and the number of model parameters a 10% weight [29].

The values of each option for the following three criteria are (Tables 19.4 and 19.5):

Table 19.4 Values of the options for the three criteria of the MCA

	P3 speed (V/s)	R2 speed (V/s)	No. of parameters
Shepherd	0.002973	0.000007	5
Thévenin	0.010944	0.017025	4
Second order RC	0.011295	0.025271	6
Third order RC	0.011383	0.02605	8
Fourth order RC	0.011446	0.026482	10

Table 19.5 The performance matrix of the MCA

	Score speed of the model	Score mean relative error	Score no. of parameters	Total
Shepherd	11.68725	0.0118947	8	19.69915
Thévenin	43.02662	28.929813	10	81.95643
Second order RC	44.40408	42.942079	6.66	94.00616
Third order RC	44.7495	44.264512	5	94.01401
Fourth order RC	45	45	4	94

Through the standardization of these values and applying the weights, the performance matrix of the MCA is obtained.

Analyzing the scores in the performance matrix, it can be noticed that the four models based on electric circuits are very similar in terms of performance, while the Shepherd model does not perform so well for this discharge profile.

Even though the fourth order RC network has the highest score regarding performance, it fails to compensate the large number of parameters used, so ends up on the third place with a total score of 94 points. Even if the score difference between the first two models is very small, **the third order RC network model**, which obtained the best score, i.e. 94.01, is the optimal model for a LFP cell subjected to discharge after the UDDS cycle, as it manages to achieve the best compromise between approximating the experimental data and the number of parameters required for modelling.

In order to validate the proposed method, we compared the data obtained from the five models subjected to discharge after the UDDS cycle to the data obtained from a LFP cell subjected to discharge after the same test—Fig. 19.9.

Once all data has been processed, the mean and maximum relative errors generated by the five models were counted. The most significant errors were reported

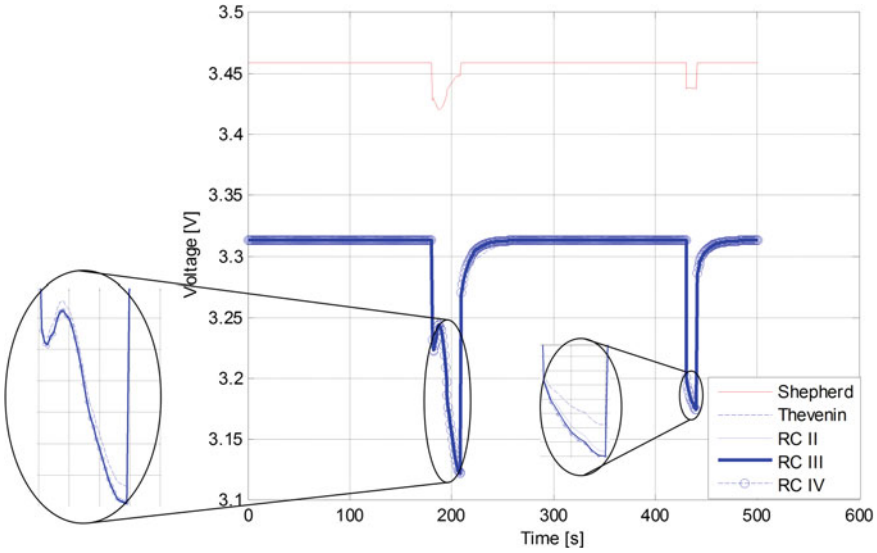

Fig. 19.8 Determining the response speed of the five models

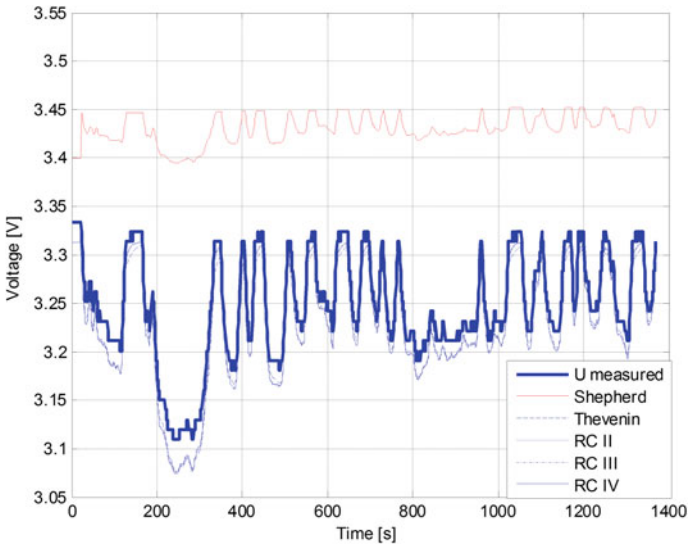

Fig. 19.9 Validating the proposed methodology

for the Shepherd model, i.e. 5.64% for the mean relative error, and 9.25% for the maximum relative error, respectively. The models based on electric circuits came within a much narrower error range, i.e. 0.53–0.57% for the mean relative error, and 1.30–1.40% for the maximum relative error, respectively. As expected the fourth

order RC network model produces the smallest errors 0.53 and 1.30% respectively, but its large number of parameters and the close performance of the other two models makes him the third choice. The third and second order RC network models have almost the same mean error of 0.55%, but the difference in the maximum error i.e. 1.34% for the third order RC network and 1.37% for the second order RC network makes the third order RC network model the best choice for this application. The results obtained from the real data comparison are very similar with the ones from the proposed methodology and so the method is validated.

19.6 Conclusions

Battery modelling is a complex area where there is still no universally valid constant. Choosing the right model is be based on several parameters, out of which the most important ones are: the range of application, the accuracy and the model complexity.

The main modeling techniques are involve electrochemical phenomena, electrical and electronic circuits or analytic approximation techniques.

The electrochemical models are based on a linear system of equations that describe the electrochemical phenomena that occur within the batteries. Solving this system require a range of techniques for approximation and reduction, which do not significantly affect the accuracy of the model, but do not significantly reduce its complexity either.

In general, the electrochemical models have high accuracy, but require large simulation periods of time and detailed knowledge about the electrochemical structures of the batteries being modelled.

The analytical models describe the behaviour of the battery at a higher abstraction level than do the electrochemical models. They have been developed from experimental tests performed on the batteries, on which curve fitting techniques were applied. The great advantage of these models is that they manage to describe the behaviour of the battery using a small number of equations. The accuracy of these models is smaller than that of the electrochemical models, but they are more suitable for incorporation into the simulation systems and other systems.

The models based on electrical circuits do not represent the internal structure of the battery, but they rather replicate its behavior by using different electrical components. They typically use voltage sources, resistors and capacitors to model the variation of the output voltage for a specific discharge profile and SoC. They have a lower degree of accuracy, but are the easiest to integrate into the simulation systems and BMSs, which makes them attractive both for battery manufacturers and developers of systems for the automotive industry.

For applications that involve rapid discharge current variations, and also periods of stability, such as the UDDS discharge profile, after the research conducted it was determined that the optimal model for an LFP cell is the **third order RC network**

model. This model was chosen from a wide range of models based on electric circuits and analytical models, using a new test methodology that was validated experimentally.

References

1. Chiasserini C, Rao RR (2001) Energy efficient battery management. IEEE J Sel Areas Commun 19(7):1235–1245
2. Pattipati BR, Sankavaram C, Pattipati KR (2011) System identification and estimation framework for pivotal automotive battery management system characteristics. IEEE Trans Sys Man Cybern Part C 11:869–884
3. Seaman A, Dao TS, McPhee J (2014) A survey of mathematics-based equivalent-circuit and electrochemical battery models for hybrid and electric vehicle simulation. J Power Sour 256:410–423
4. Wua B, Mohammedb M, Brighamb D, Elderb R, White RE (2001) A non-isothermal model of a nickel—metal hydride cell. J Power Sour 101(2):149–157
5. Suleiman A-S, Dennis D (2004) Rapid test and non-linear model characterisation of solid-state lithium-ion batteries. J Power Sour 130(1–2):266–274
6. Kim MJ, Peng HB, Lin C-C, Stamos E, Tran D (2005) Testing, modeling, and control of a fuel cell hybrid vehicle. In: ACC Conference, Portland, OR, United States, vol 6. Article number FrA14.3, pp 3859–3864
7. Enache B, Lefter E, Cepișcă C (2014) Autonomous vehicles: intelligent transport systems and smart technologies, Chap. 15. Batteries for electrical vehicles: a review. Nova Science Publishers Inc., pp 323–345
8. Fuller TF, Doyle M, Newman J (1994) Simulation and optimization of the dual lithium ion insertion cell. J Electrochem Soc 141(1):1–10
9. Forman JC, Moura SJ, Stein JL, Fathy HK (2012) Genetic identification and fisher identifiability analysis of the Doyle–Fuller–Newman model from experimental cycling of a $LiFePO_4$ cell. J Power Sour 210:263–275
10. Albertus P, Newman J (2014) Introduction to Dualfoil 5.0. http://www.cchem.berkeley.edu/jsngrp/fortran_files/Intro_Dualfoil5.pdf. Accessed 29 May 2014
11. Doerffel D, Suleiman A-S (2006) A critical review of using the peukert equation for determining the remaining capacity of lead-acid and lithium-ion batteries. J Power Sour 155:395–400
12. Pavlov D, Petkova G (2002) Phenomena that limit the capacity of the positive lead acid battery plates: I. The charge potential transient as an indicator of positive plate state of charge and state of health. J Electrochem Soc 149:A644–A653
13. Pavlov D, Petkova G (2002) Phenomena that limit the capacity of the positive lead acid battery plates: II. Electrochemical impedance spectroscopy and mechanism of discharge of the plate. J Electrochem Soc 149:A654–A661
14. Hausmann A, Depcik C (2013) Expanding the peukert equation for battery capacity modeling through inclusion of a temperature dependency. J Power Sour 235:148–158
15. Shepherd CM (1965) Design of primary and secondary cells II. An equation describing battery discharge. J Electrochem Soc 112:657–664
16. Tremblay O, Dessaint LA, Dekkiche AI (2007) A generic battery model for the dynamic simulation of hybrid electric vehicles. In: VPPC conference, pp 284–289
17. Enache B, Lefter E, Stoica C (2013) Comparative study for generic battery models used for electric vehicles. In: Proceedings of the 8th international symposium on advanced topics in electrical engineering, pp 1–6

18. Li J, Mazzola MS (2013) Accurate battery pack modeling for automotive applications. J Power Sour 237:215–228
19. Huria T, Ceraolo M, Gazzarri J, Jackey R (2012) High fidelity electrical model with thermal dependence for characterization and simulation of high power lithium battery cells. In: IEVC conference, pp 1–8
20. Wang L, Cheng Y, Zou J (2014) Battery available power prediction of hybrid electric vehicle based on improved dynamic matrix control algorithms. J Power Sour 261:337–347
21. Jackey R, Saginaw M, Gazzarri J, Huria T, Ceraolo M (2013) Battery model parameter estimation using a layered technique: an example using a lithium iron phosphate cell. https://www.mathworks.com/tagteam/76117_SAE%203013%20-%20Battery%20Estimation%20Layered%20Technique.pdf. Accessed 01 Sept 2015
22. Verbrugge B, Heremans Y (2009) Modelling the RESS: describing electrical parameters of batteries and electric double-layer capacitors through measurements. World EVJ 3
23. Hariharan SK, Kumar VS (2013) A nonlinear equivalent circuit model for lithium ion cells. J Power Sour 222:210–217
24. Lefter E, Enache B, Mara I, Goia C (2015) Hybridization of trolleybuses—means for increasing the transports flexibility and reduction of the pollution. UPB Sci Bull Ser C 77 (3):293–304
25. Enache B, Constantinescu LM, Alexandru ME (2015) A $LiFePO_4$ battery discharge simulator for EV applications—part 2: developing the battery simulator. In: Proceedings of the 9th international symposium on advanced topics in electrical engineering, pp 883–888
26. USCAR (1996) USABC electric vehicle battery test procedures manual, revision 2
27. PNGV (2001) PNGV battery test manual, revision 3
28. Duong T (2000) USABC and PNGV test procedures. J Power Sour 89:244–248
29. Enache B, Constantinescu LM, Alexandru ME (2015) A $LiFePO_4$ battery discharge simulator for EV applications—part 1: determining the optimal circuit based battery model. In: Proceedings of the 9th international symposium on advanced topics in electrical engineering, pp 877–882
30. Pistoia G (2014) Lithium-ion batteries advances and application, Chap. 4. In: Hudak N (ed) Nanostructured electrode materials for lithium-ion batteries. Elsevier, pp 57–82